

Effect of NH_4I and I_2 concentration on agar gel polymer electrolyte properties for a dye-sensitized solar cell

Siti Salwa Alias · Ahmad Azmin Mohamad

Received: 17 September 2012 / Revised: 6 November 2012 / Accepted: 9 December 2012 / Published online: 21 December 2012
© Springer-Verlag Berlin Heidelberg 2012

Abstract Gel polymer electrolytes were prepared using agar polymer host, NH_4I , and I_2 salts. The sample of agar paste with 1.0 M of NH_4I and 0.2 μM of I_2 exhibits the highest conductivity and lowest viscosity values at room temperature of $(2.64 \pm 0.19) \times 10^{-3} \text{Scm}^{-1}$ and $1.17 \pm 0.29 \text{Pas}$, respectively. All of the gel polymer electrolytes display Arrhenian behavior, and the optimum agar paste gave the lowest activation energy of 0.25 eV. It also had a good physical appearance compared with the other samples. This gel polymer electrolyte had a good potential and was applicable to a role as electrolyte in ITO-ZnO (N719 dye)/agar paste+1.0 M NH_4I +0.2 μM I_2 /Au-Pd-ITO dye-sensitized solar cell.

Keywords Agar gel · Polymer electrolyte · Ammonium iodide · Iodine · Dye sensitized solar cell

Introduction

The dye-sensitized solar cell (DSSC) was developed by Honda and Fujishima [1] by introducing a nanostructured semiconductor, dye sensitization, and a reduction and oxidation (redox) electrolyte. Grätzel and co-workers [2, 3] used a nanoporous structure with a large-surface-area titanium oxide (TiO_2) thin-film electrode, a novel Ru bipyridyl complex as the dye, and an iodide/triiodide (I^-/I_3^-) couple as the redox electrolyte for DSSC fabrication. Zinc oxide (ZnO) is another attractive semiconductor material that has been used extensively for DSSC applications. One work showing excellent performance of a DSSC using ZnO as a working electrode was presented by Saito and Fujihara [4].

The use of liquid electrolyte is considered one of the techniques to improve the contact between the working electrode, the electrolyte, and the counter electrode. The existence of an optimal contact surface for the (I^-/I_3^-) redox electrolyte gives the best DSSC performance [5]. However, liquid electrolytes have several drawbacks, such as leakage, volatilization of the liquid, possible desorption and photo degradation of the attached dyes, and corrosion of the counter electrode. These shortcomings hinder their practical application and limit the long-term performance of DSSCs [6, 7]. A quasi-solid-state DSSC was developed by using a gelator to replace liquid electrolytes to solve the leakage problem. Gelation can be accomplished by adding gelator into the electrolyte [8]. In addition, the development of gel polymer electrolyte (GPE) could be used to overcome this problem. Kubo et al. [7] developed the quasi-solid-state DSSC by using gelator. This DSSC performance with GPE was comparable with DSSC using liquid electrolyte studied by Keis et al. [9].

Recently, biopolymer materials, such as chitosan, agarose, and carrageenan, have been used extensively as DSSC electrolytes [10–14]. Agar and carrageenan are other biopolymers that can possibly be used in the fabrication of DSSCs. Agar and carrageenan are in a class of marine algae biopolymers extracted from red seaweed polysaccharides and are hydrophilic in nature [15], while konnyaku (konjac glucomannan gel) is a polysaccharide that is elastic and insoluble in water [16]. Konnyaku has been used to interact synergistically with other hydrocolloids such as carrageenan [17, 18]. These three kinds of polysaccharides are usually blended together and are known commercially as agar-agar. Figure 1 illustrates the structure of agar and carrageenan. The previous study on biopolymer materials has been revealed that conductivity values of agarose and κ -carrageenan electrolyte for the PEC were 4.36 and $2.82 \times 10^{-3} \text{Scm}^{-1}$, respectively. These conductivity values are compared to the conductivity value of liquid electrolyte ($4.40 \times 10^{-3} \text{Scm}^{-1}$) for the DSSC application [13].

S. S. Alias · A. A. Mohamad (✉)
School of Materials and Mineral Resources Engineering,
Universiti Sains Malaysia, 14300, Nibong Tebal,
Penang, Malaysia
e-mail: azmin@eng.usm.my

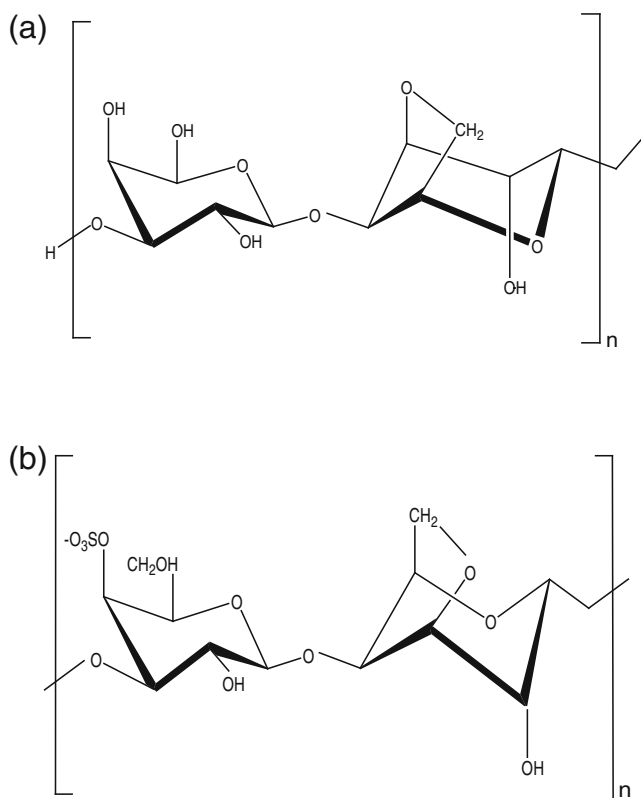


Fig. 1 Structure of **a** agar and **b** carrageenan

In general, the enhancement of the DSSC performance also depends on counter cations of iodides salts in electrolyte, such as Li^+ , Na^+ , K^+ , and R_4N^+ [19–21]. These counter cations owe the different ionic conductivities from the electrolyte or adsorption on the oxide semiconductor surface. Thus, the counter cations lead to a shift in the conduction band level of the oxide semiconductor electrode [22]. The DSSC electrolyte also needs Γ/I_3^- redox ions to reduce the oxidized dye and functions as the charge carrier mediator in the regenerative DSSC. Hence, both inorganic and organic iodide salts have significant influence on the performance of the DSSC [6].

Ammonium iodide (NH_4I) is presented as one of the alkali iodide besides LiI/I_2 [20, 21]. NH_4I has potential to be used as salt in polymer electrolyte together with I_2 , particularly for the DSSC electrolyte. The complex of polyethylene oxide (PEO) with NH_4I salt film demonstrated a good ionic conductivity within a range of $\sim 10^{-5} \text{Scm}^{-1}$ [23]. In fact, PEO–chitosan complex with $\text{NH}_4\text{I} + \text{I}_2$ has been employed as electrolyte for the DSSC. Based on these previous studies, the ionic conductivity of the polymer electrolyte attained was $8.47 \times 10^{-4} \text{Scm}^{-1}$ [10, 14, 24].

Because there has been no systematic research on DSSCs based on ZnO working electrodes and agar complexes with NH_4I and I_2 (Γ/I_3^-) redox electrolytes, the aim of this study was to examine the properties of DSSCs using GPE and

ZnO as the working electrode. The GPEs were based on agar, ammonium iodide (NH_4I), and iodine (I_2) as the redox electrolyte. The agar paste GPE with the highest conductivity was then used to fabricate an ITO–ZnO (N719 dye)/GPE/Au–Pd–ITO DSSC, and its performance was measured.

Experimental

Agar paste + $\text{NH}_4\text{I} + \text{I}_2$: preparation and characterization

GPE was prepared by mixing 1.0 g of agar powder (BITES, Jim-Willie, Singapore) with 20 ml glycerol (Merck). The mixture was boiled at 80 °C for 15 min. The gel was left at 25 °C for 15 min for the gelation and cooling process. Next, the GPE preparation and characterization processes were split into two parts. For the first part, agar paste was mashed briskly. Various concentrations of NH_4I (Sigma-Aldrich) salt from 0.2 to 2.0 M were added to the agar paste. Electrochemical impedance spectroscopy was used to determine the conductivity. A sample of agar paste was placed in the spacer between stainless steel (SS) block electrodes inside the Teflon cell. This cell was connected to an Autolab PGSTAT 30 frequency response analyzer (Eco Chemie B.V.) with a frequency range of 0.1 Hz to 1.0 MHz and an amplitude of 10 mV.

For the second part, the most conductive agar paste with NH_4I and good physical properties was then doped with various concentrations of iodine solution (I_2 , Aldrich) from 0.1 to 0.4 μM to complete the GPE preparation process. The viscosity (η) was determined using a Haake Viscotester VT550. The viscosity values were calculated from the graph of η as a function of time (t). Then, the variation of the viscosity and conductivity of the agar paste GPE at room temperature was plotted.

The conductivity of the GPE at elevated temperatures was measured in a temperature range from 25 to 120 °C. The physical appearances of the agar paste GPE were investigated with a stereo zoom microscope with magnification of $\times 4.0$.

Dye-sensitized solar cell: device fabrication and characterization

Conducting indium tin oxide (ITO) glass with a sheet resistance of $8 \Omega \text{cm}^{-2}$ was used. The ZnO powder was prepared earlier by the sol–gel method [25]. ZnO powder (0.5 g) was ground with acetic acid (0.035 M) (CH_3COOH , Merck) and a few drops of Triton X-100 emulsification agent ($\text{C}_{14}\text{H}_{22}$ ($\text{C}_2\text{H}_4\text{O}$)N, Sigma-Aldrich). The prepared ZnO paste was then spread on the ITO glass with an active area of 1cm^2 . Then, sintering was carried out at 400 °C for 30 min in a furnace. The ZnO working electrode was left to cool prior to being dipped in 0.5 mM of dye, *cis-bis*(isothiocyanato) *bis*

(2,2'-bipyridyl-4,4'-dicarboxylato)-ruthenium (II) bis-tetra-butylammonium (N-719) (Aldrich), for 1 h.

For the counter electrode, the conductive side of the ITO glass was coated with gold–palladium (Au-Pd) in the setup. Next, the agar paste GPE with the highest conductivity was placed in the space between the working electrode and counter electrode as shown in Fig. 2.

The performance of the ITO-ZnO (N719 dye)/GPE/Au-Pd-ITO cell was characterized by measuring the current density-voltage (J - V) under illumination and dark condition by connecting the cell to Autolab PGSTAT 30 GPES software (Eco Chemie, B.V.). The illumination test was carried out using a halogen lamp by Philips (120 V; 50 W) with a light intensity of 100 mWcm^{-2} . The open circuit voltage (V_{OC}), short circuit current density (J_{SC}), maximum voltage (V_{max}), and maximum current density (J_{max}) were calculated based on the X - Y -axis intercepts and the square area under the J - V curves.

Results and discussion

Agar paste + NH_4I + I_2 : A Nyquist plot

Selected Nyquist plots of the agar paste with different NH_4I and I_2 concentrations are shown in Fig. 3. The intersection of the imaginary axis with the real axis provides the value of R_b . The R_b value for pure agar paste was $1,341.60 \Omega$ (Fig. 3a). Figure 3b, c show the Nyquist plots for agar paste with 0.2–1.0 M of NH_4I and 1.2–2.0 M of NH_4I , respectively. The value of R_b decreases proportionally with the addition of NH_4I .

The Nyquist plot of the agar paste as a function of 1.0 M of NH_4I and various concentrations of I_2 is shown in Fig. 3d. There is no existing capacitance component. All agar pastes show only a resistive component due to the effect of adding a high I_2 concentration. The R_b value decreases for 0.1 and 0.2 μM of I_2 . However, the R_b value increases for the agar paste with 0.3 and 0.4 μM of I_2 . Based on the Nyquist plot results, agar paste+1.0 M of NH_4I +0.2 μM of I_2 gives the lowest R_b value of 75.04Ω for the GPE system.

The trend of the agar paste Nyquist plot is close to the trend observed in a system using glycerol as an organic

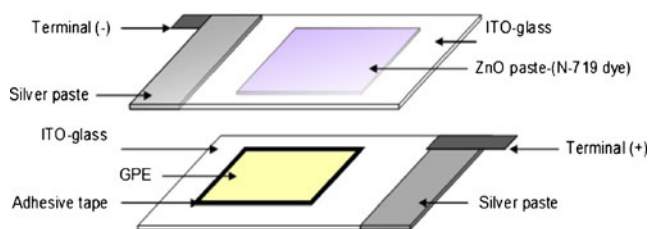


Fig 2 Schematic diagram of photoelectrochemical cell components

solvent [26]. The small curve observed at the beginning of the agar paste plot shows the capacitive behavior at higher frequency ranges. The conductive charge carriers cannot easily cross the electrodes/electrolyte and form the curve. The concentration gradients of conductive charge carriers increase and gather near the interface of SS electrodes when an electric field is applied, which impedes the further diffusion of conductive charge carriers until an equilibrium state is reached [26, 27]. Besides that, the disassociation of NH_4I and I_2 provided a constant amount of I^- and I_3^- similar with study done by Tan et al. [28]. Thus, this can form an ordinary form of GPE. The continuous decreased of bulk resistance could be noticed when more I_2 diffused into the agar paste network at optimum concentration. Nevertheless, the bulk resistance increased at 0.3 and 0.4 μM of I_2 . This attributed by the excessive amount of I_2 . At these concentrations, I_2 cannot diffuse into agar paste network straightforwardly.

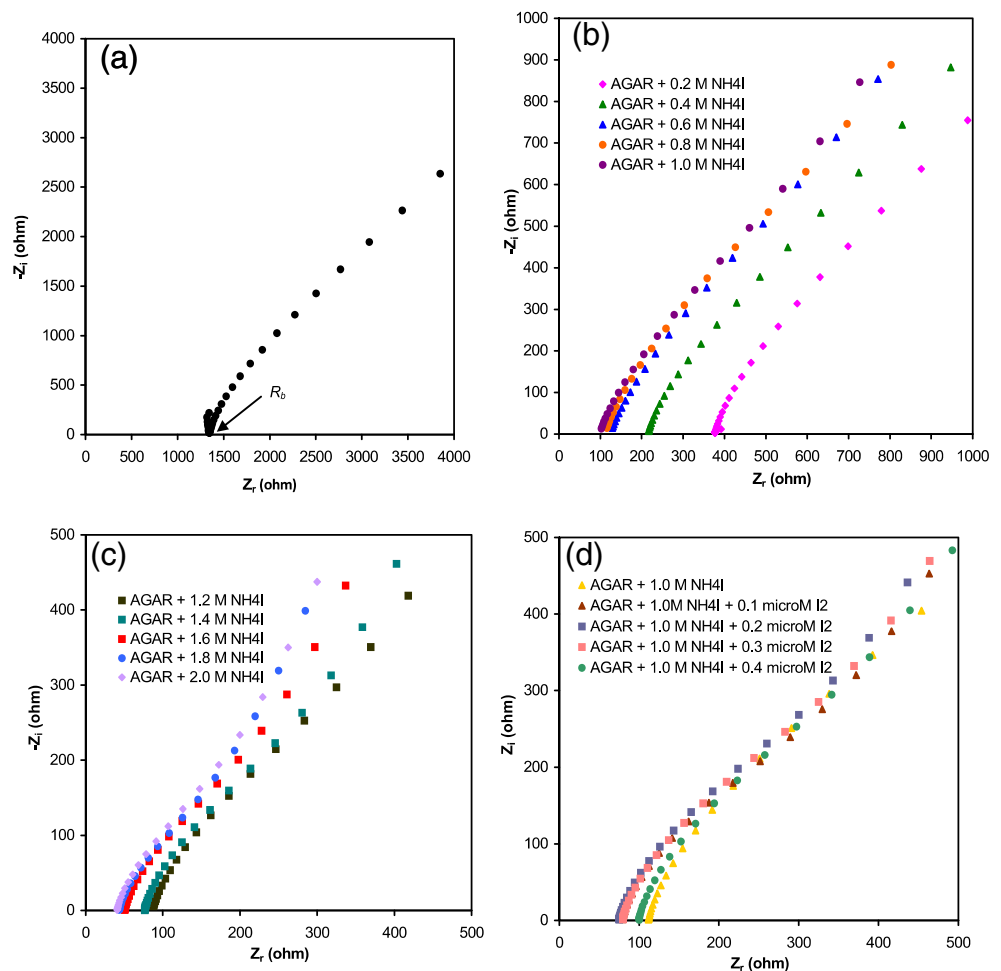
Agar paste + NH_4I + I_2 : conductivity and viscosity

Figure 4 shows the conductivity and viscosity values of agar paste as a function of NH_4I concentrations. The conductivity of pure agar paste coded as A was $(1.50 \pm 0.25) \times 10^{-4} \text{ Scm}^{-1}$. The conductivity increased slightly when 0.2 M of NH_4I was added to the sample. When the concentration of NH_4I was increased to 0.4 M, the conductivity value of the agar paste continued to increase. The increase in conductivity remained constant when 0.6, 0.8, and 1.0 M of NH_4I were added to the agar paste, as plotted in region 1. The conductivity increased slightly in region 2 compared to region 1. The conductivity values continued to increase with NH_4I concentration for the agar pastes with 1.2 to 1.8 M of NH_4I . The agar paste with 2.0 M of NH_4I had the highest conductivity value of $(4.89 \pm 0.62) \times 10^{-3} \text{ Scm}^{-1}$.

In the viscosity measurement, the agar paste had the highest viscosity value at $(11.43 \pm 3.97) \text{ Pas}$. The viscosity decreased slightly and continuously for 0.2–1.0 M of NH_4I , as shown in region 1. In region 2, when the NH_4I concentration increased to 1.2–1.8 M, the viscosity continued to decrease steadily. The lowest viscosity, $(2.67 \pm 0.29) \text{ Pas}$, was obtained in samples coded as A2.0N. The values of the conductivity and viscosity of agar paste with various concentrations of NH_4I are tabulated in Table 1. The agar paste with 1.0 M of NH_4I (A1.0N) was chosen as the optimum composition based on the trade-off between conductivity and viscosity values for the next step.

Meanwhile, the relation between the conductivity and viscosity values of the agar paste as a function of the optimum conductivity using 1.0 M of NH_4I with various concentrations of I_2 is shown in Fig. 5. The trend of the conductivity curve increased slightly for A1.0N.0.11 and

Fig. 3 Complex impedance plot of **a** agar paste (agar + glycerol), **b** agar paste+0.2–1.0 M of NH_4I , **c** agar paste+1.0–2.0 M of NH_4I , and **d** agar paste+1.0 M of NH_4I +different concentrations of I_2



gave the highest conductivity value of $(2.64 \pm 0.19) \times 10^{-3} \text{ S cm}^{-1}$ for A1.0N0.2I. However, starting with A1.0N0.3I, the conductivity value decreased. Concurrently, when $0.1 \mu\text{M I}_2$ was added to A1.0N, the viscosity value suddenly decreased. After reaching the lowest viscosity value, the viscosity values increased abruptly for A1.0N0.3I and A1.0N0.4I. The lowest viscosity was noted in A1.0N0.2I with a value of $(1.17 \pm 0.29) \text{ Pa s}$. Table 2 lists the values of the conductivity and viscosity of the optimum composition A1.0N with various I_2 concentrations.

The conductivity of the agar paste was inversely proportional to the viscosity when NH_4I and I_2 concentrations increased. This result is also in accordance with that of Bonhote et al. [29], in terms of the conductivity being inversely proportional to the viscosity based on iodide as a type of salt. The increase in the conductivity values is attributed to the increasing amount of charge carriers (H^+ and Γ) in the samples. Even though the main focus of this work was Γ and I_3^- as the main species for DSSC, the contribution of H^+ to the conductivity cannot be ruled out. Nevertheless, the conductivity values in this study decreased with the addition of 0.3 and $0.4 \mu\text{M}$ of I_2 , which was

attributed to ion-pairing phenomena. Excess I_2 initially becomes Γ/I_3^- . A free iodide from NH_4I forms a triiodide

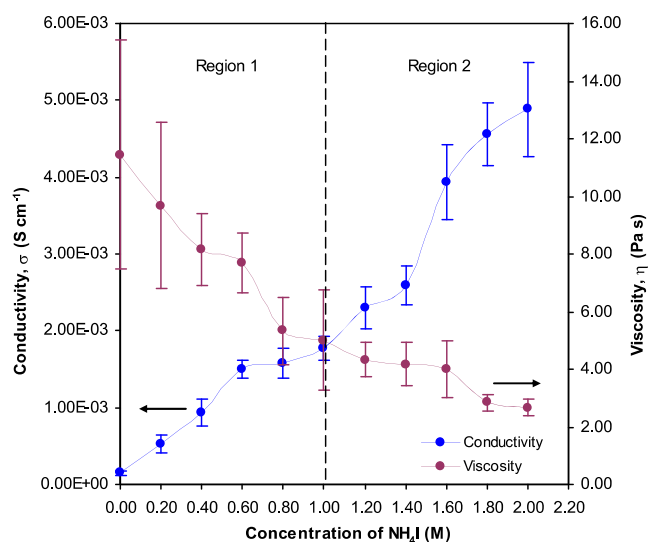


Fig. 4 Relation of conductivity and viscosity of agar paste in different concentrations of NH_4I

Table 1 Conductivity and viscosity of agar paste at different NH₄I concentrations

Sample name	Agar (g)	Glycerol (ml)	NH ₄ I concentration (M)	Conductivity, σ (S cm ⁻¹)	Viscosity, η (Pa s)
Pure agar (A)	1.0	20	0.0	$(1.50 \pm 0.25) \times 10^{-4}$	11.43 ± 3.97
A0.2N	1.0	20	0.2	$(5.24 \pm 1.11) \times 10^{-4}$	9.67 ± 2.89
A0.4N	1.0	20	0.4	$(9.39 \pm 1.75) \times 10^{-4}$	8.17 ± 1.26
A0.6N	1.0	20	0.6	$(1.49 \pm 0.12) \times 10^{-3}$	7.67 ± 1.04
A0.8N	1.0	20	0.8	$(1.58 \pm 0.19) \times 10^{-3}$	5.33 ± 1.15
A1.0N	1.0	20	1.0	$(1.77 \pm 0.16) \times 10^{-3}$	5.00 ± 1.73
A1.2N	1.0	20	1.2	$(2.29 \pm 0.27) \times 10^{-3}$	4.33 ± 0.58
A1.4N	1.0	20	1.4	$(2.59 \pm 0.25) \times 10^{-3}$	4.17 ± 0.76
A1.6N	1.0	20	1.6	$(3.94 \pm 0.48) \times 10^{-3}$	4.00 ± 1.00
A1.8N	1.0	20	1.8	$(4.56 \pm 0.41) \times 10^{-3}$	2.83 ± 0.29
A2.0N	1.0	20	2.0	$(4.89 \pm 0.62) \times 10^{-3}$	2.67 ± 0.29

(I₃⁻) with the iodine according to the reduction process as follows:



The increase of I⁻ to I₃⁻ (higher concentration of polyiodide ions) enhances the ability of anions to hop along with H⁺ to the coordinate sites [30, 31]. Thus, the value of the agar paste conductivity increased. However, the charge carrier (H⁺ and I₃⁻) ion pairing occurred upon the addition of 0.3 and 0.4 μM of I₂. The number of anion (I₃⁻) charge carriers in the agar paste decreased in proportion to the conductivity.

The continuous decrease of the viscosity values with increasing NH₄I concentration in this work demonstrates that the viscosity is strongly dependent on the salt concentration. The NH₄I concentration contributes to the frictional force between the constituent ions (H⁺ and I⁻) [32]. Thus, the increase in the NH₄I concentration reduced the friction force of H⁺ and I⁻ along the agar structure backbone. Subsequently, both of these ions can enter the agar paste, move along easily, and separate the agar structure backbone chains, reducing the viscosity value.

Furthermore, the increase of I⁻ to I₃⁻ in A1.0N0.1I and A1.0N0.2I reduced the viscosity values, which was similar to what happened for the agar paste + NH₄I in various concentrations. The decrease in viscosity could be the reason why the conductivity of the samples increased slightly. In contrast, the viscosity values suddenly increased with increasing concentrations of I₂ to 0.3 and 0.4 μM. At this point, the high concentrations of I₂ increased the friction force of paired ions inside the agar paste. In addition, Renard et al. [33] found that an increase of I₃⁻ ion pairing contributed to increased viscosity values. The conductivity values of GPE in this work were almost similar (~10⁻³ S cm⁻¹) with those reported in a previous work on electrolyte based on biopolymer (~10⁻⁶ to 10⁻⁴ S cm⁻¹) [10, 24],

agarose (10⁻⁴ to 10⁻³ S cm⁻¹) [20, 21], and agar and carrageenan (10⁻³ S cm⁻¹) [34] for DSSCs.

Agar paste + NH₄I + I₂: conductivity–thermal dependence behavior

The temperature dependences for A, A1.0N, A1.0N0.1I, A1.0N0.2I, and A1.0N0.3I at a temperature range of 298 to 393 K are shown in Fig. 6. The conductivity of samples increased proportionally to the temperature and showed an Arrhenius type relation. The pure agar paste had the lowest conductivity compared with the other samples. The conductivity increased slightly in A1.0N compared with the pure agar paste. When 0.1 and 0.2 μM of I₂ were added to the agar paste +1.0 M NH₄I samples, the conductivity became higher. Conversely, the conductivity decreased for A1.0N0.3I.

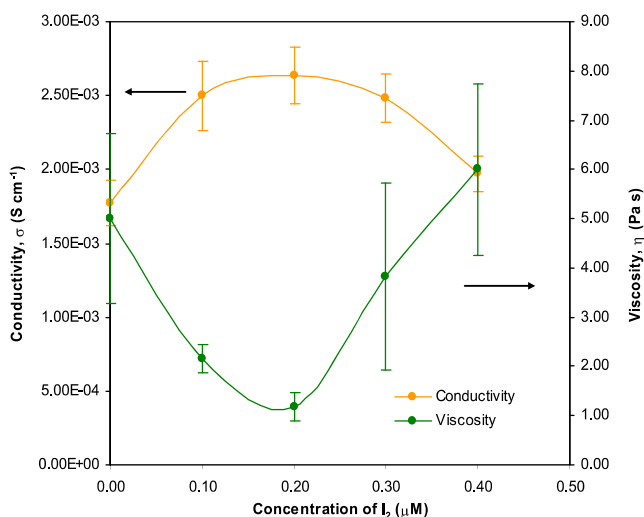


Fig. 5 Relation of conductivity and viscosity of agar paste+1.0 M of NH₄I+different concentrations of I₂

Table 2 Conductivity and viscosity of A1.0N with different I₂ concentrations

Sample name	I ₂ concentration (μM)	Conductivity, σ (Scm ⁻¹)	Viscosity, η (Pas)
A1.0N	0	$(1.77 \pm 0.16) \times 10^{-3}$	5.00 ± 1.73
A1.0N0.1I	0.1	$(2.50 \pm 0.23) \times 10^{-3}$	2.17 ± 0.29
A1.0N0.2I	0.2	$(2.64 \pm 0.19) \times 10^{-3}$	1.17 ± 0.29
A1.0N0.3I	0.3	$(2.48 \pm 0.16) \times 10^{-3}$	3.83 ± 1.89
A1.0N0.4I	0.4	$(1.97 \pm 0.12) \times 10^{-3}$	6.00 ± 1.73

There was no sudden change in the value of conductivity with temperature because these complexes do not undergo any phase transitions within this temperature range. Normally, the polymer matrix is amorphous and has large amounts of free volume cages [35]. Thus, as the temperature increases, the agar paste samples can expand easily and produce free volume proportionally to the overall mobility of H⁺ and I⁻ ions along the agar backbone chain [36]. Moreover, the segmental mobility assists ion transport. Therefore, the retarding effect of the ion clouds almost balances [37]. However, the increasing ion association decreased the free volume amount even at elevated temperature for A1.0N0.3I. At this stage, the lower fraction of free volume was no longer balanced as the number of anion charge carriers (I₃⁻) was continuously increased. As a result, the conductivity decreased with increasing I₂ concentration at elevated temperatures. The conductivity values are almost similar to those reported in previous studies on GPE temperature dependence plots [35, 38, 39].

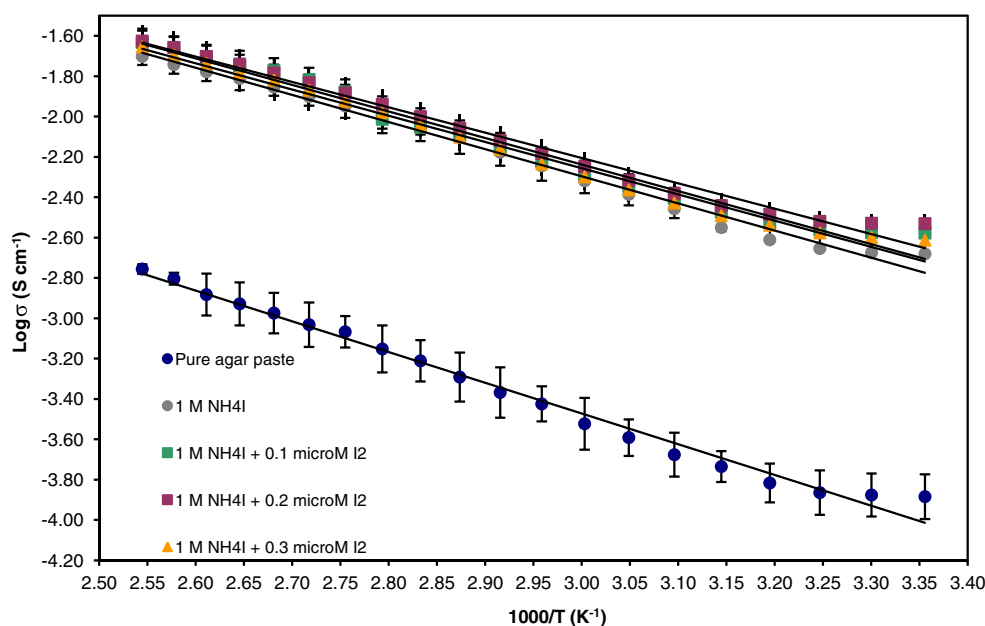
The relationship of the variation of the activation energy and conductivity at room temperature is shown in Fig. 7. The activation energy of pure agar paste, A1.0N, A1.0N0.1I,

A1.0N0.2I, and A1.0N0.3I at room temperature was calculated from the linear temperature dependence plot in Fig. 6. The highest activation energy value was 0.30 eV for pure agar paste. The activation energy value decreased slightly for A1.0N and A1.0N0.1I. The lowest activation energy, found for A1.0N0.2I, was 0.25 eV. However, when the I₂ concentration increased to 0.3 μM in A1.0N0.3I, the activation energy value increased. The variations of the activation energy values were inversely proportional to the conductivity. The results of the activation energy values for agar paste samples with different I₂ concentrations are summarized in Table 3.

The variation of activation energy values was influenced by the different concentrations of I₂. The conductivity of agar paste+1.0 M NH₄I+different concentrations of I₂ decreased slightly after reaching a maximum conductivity, which is attributed to the increase of the redox couple species (I₃⁻) at high I₂ concentrations. Therefore, the conductivity values increased when the I₂ concentration increased to 0.1 and 0.2 μM. Concurrently, the activation energies needed for the H⁺ and I₃⁻ ions to hop together on the coordinating site of the agar were lower compared with those of the pure agar paste and A1.0N. Nonetheless, conductivity decreased, and the activation energy value increased for A1.0N0.3I, which is attributed to the ion pairing in agar paste. Thus, the hopping mechanism of H⁺ and I₃⁻ ions occurred with a high activation energy value at the agar coordinating site.

Agar paste + NH₄I + I₂: physical properties

The images of agar powder transformed to agar paste when glycerol and various concentrations of NH₄I were added are shown in Fig. 8. Figure 8a shows that agar powder has a

Fig. 6 The temperature dependence of conductivity for agar paste with NH₄I and I₂

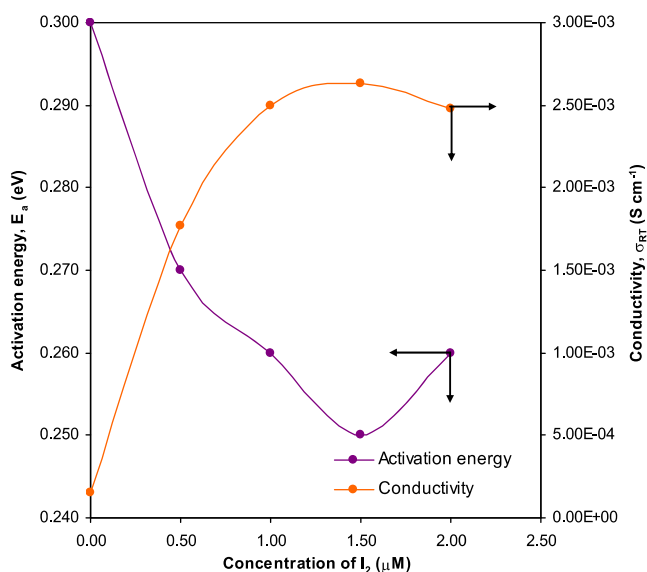


Fig. 7 Variation of activation energy and conductivity at room temperature for agar paste with NH₄I and I₂

flaky physical appearance with an average size of about 42 μm. Pure agar paste (Fig. 8b) and A0.2N (Fig. 8c) are the bulky pastes obtained after the addition of glycerol and 0.2 M of NH₄I, respectively. The agar paste changed to a clear transparent paste when the NH₄I concentrations were increased to 1.0 M (A1.0N), as shown in Fig. 8d. However, when the concentrations of NH₄I were increased from 1.4 to 2.0 M (Fig. 8e, f), NH₄I was not mixed homogeneously with the agar paste due to the “cage” phenomenon. Hence, at these concentrations, the sample showed brownish spots due to the problem of ions being encapsulated within the agar paste.

The images of agar paste+1.0 M of NH₄I with different concentrations of I₂ are shown in Fig. 9. In Fig. 9a, b, it can be observed that the images of A1.0N0.1I and A1.0N0.2I show fewer brownish spots. At this concentration of I₂, I₂ (solution) could dissolve the brownish spots of NH₄I. The formations of brownish spots shed some light on the conductivity and viscosity results. Normally, the salts (NH₄I and I₂) dissolve into gel electrolyte (agar paste). The good dissolution of salts was shown by the formation of a transparent paste.

However, in samples with high I₂ concentration (A1.0N0.3I and A1.0N0.4I), the formation of brownish spots started again (Fig. 9c, d). This second formation of brownish spots was

Table 3 The activation energy for agar paste samples

Sample name	Activation energy, <i>E_a</i> (eV)
A	0.300
A1.0N	0.270
A1.0N0.1I	0.260
A1.0N0.2I	0.250
A1.0N0.3I	0.260

mostly due to the association of I₂. Herein, when the salt reached the maximum dissociation to free charge carriers, the free charge carriers became associated again. The formation of subsequent brownish spots in this work is a physical evidence to support the reassociation of charge carriers (ion pairing). At this high concentration of I₂ and ion pairing phenomena, the salt cannot mix well with the agar paste. Hence, the brownish spots appeared clearly on agar paste surface. These results are also parallel with the conductivity and viscosity results. Based on the physical properties, A1.0N0.2I shows better physical properties, conductivity, and viscosity compared with the other samples. Hence, A1.0N0.2I was chosen as the GPE for DSSC fabrication.

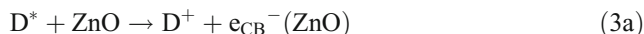
ITO-ZnO (N719 dye)/A1.0N0.2I/Au-Pd-ITO: current density-voltage

Figure 10 shows the current density-voltage curve characteristics of the DSSCs based on ITO-ZnO (N719 dye)/A1.0N0.2I/Au-Pd-ITO under an illumination of 100 mW cm⁻². Table 4 listed the J-V curve properties of PEC based ITO-ZnO (N719 dye)/A1.0N0.2I/Au-Pd-ITO under illumination of 100 mW cm⁻². Equations 2–5 represent the mechanism of ITO-ZnO (N719 dye)/A1.0N0.2I/Au-Pd-ITO. This mechanism is proposed based on the photophysical process and combined reduction and oxidation reaction in TiO₂ DSSCs discovered by Calogero and Marco [40].

The monolayer of dye (D) adsorbed chemically at the ZnO surface was irradiated by light (hν) and converted to the electronically excited state (D*). It is preferable for the excited state to lie a long way above the conduction band (CB) edge of the ZnO nanoparticles:



In this condition, the electron (e⁻) was injected into the conduction band of ZnO:



Next, to allow the reaction (Eq. 3a) to occur successfully, the electron injection process needed to compete with the deactivation reaction. Herein, the deactivation reaction is the process of reduction of D* to its origin form, D:



In order to attain a high-current generation, the oxidation of iodide [41] to triiodide (I₃⁻) in (Eq. 4a) must effectively compete with the charge-separated state during the recombination process (Eq. 4b):

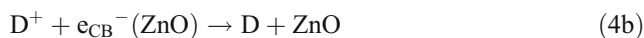
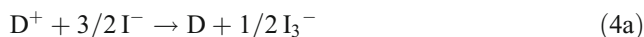
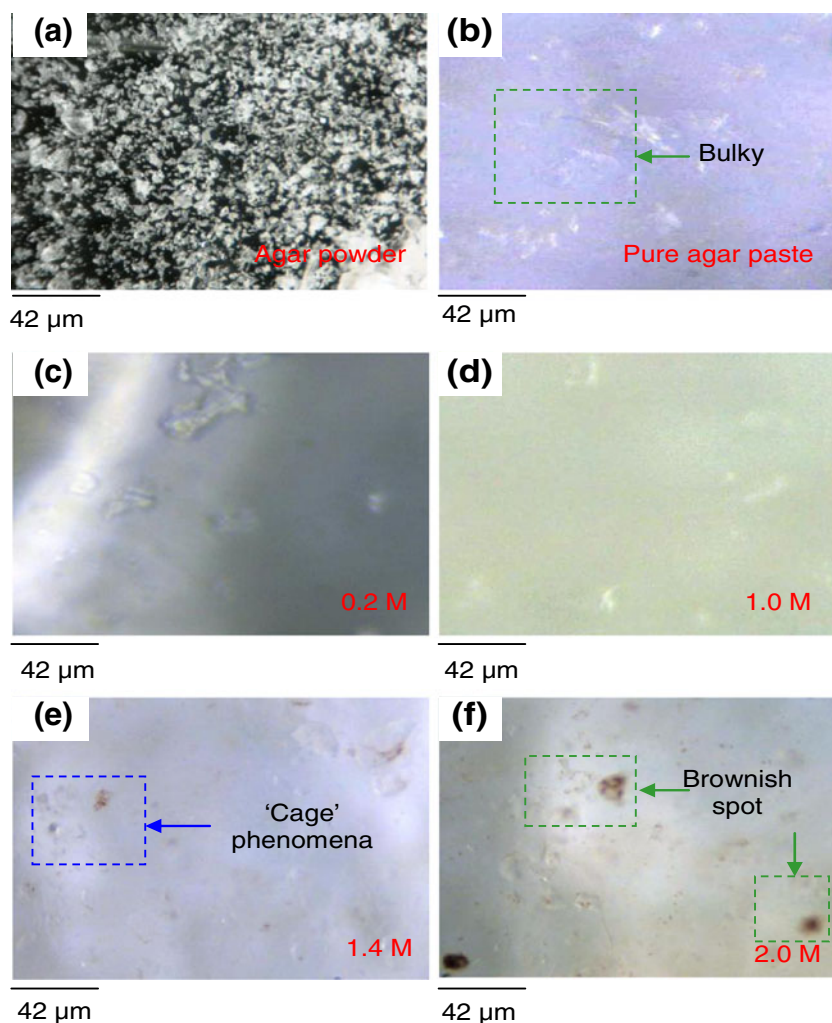


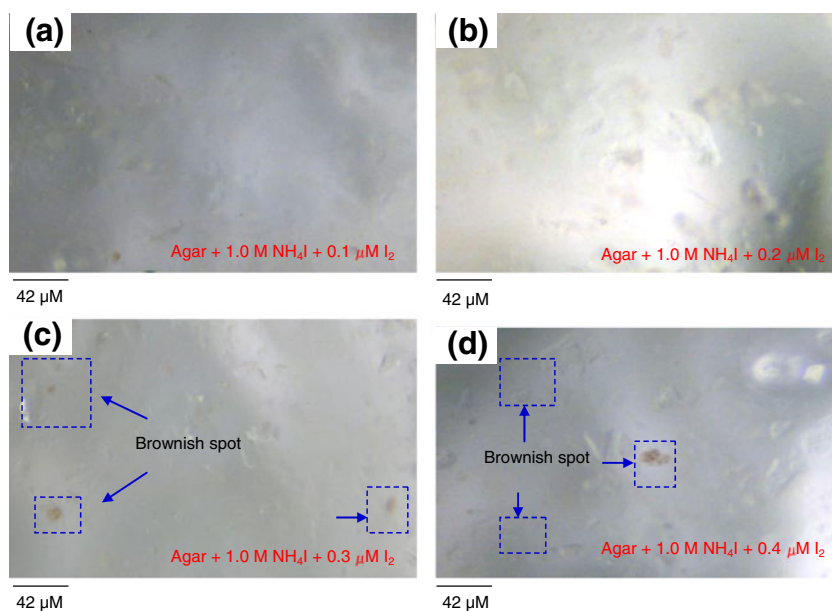
Fig. 8 Actual image of **a** agar powder, **b** pure agar paste (agar + glycerol), **c** agar paste+0.2 M NH_4I , **d** agar paste+1.0 M of NH_4I , **e** agar paste+1.4 M NH_4I , and **f** agar paste+2.0 M NH_4I



The failure of the oxidation reaction to compete with the charge-separated state will decrease the amount of current

production in DSSCs. On the other hand, the I_3^- will accept electrons from the counter electrode (Au-Pd-ITO glass) to

Fig. 9 Actual image of **a** agar paste+1.0 M NH_4I , **b** agar paste+1.0 M NH_4I +0.1 μM I_2 , **c** agar paste+1.0 M NH_4I +0.2 μM I_2 , **d** agar paste+1.0 M NH_4I +0.3 μM I_2 , and **e** agar paste+1.0 M NH_4I +0.4 μM I_2



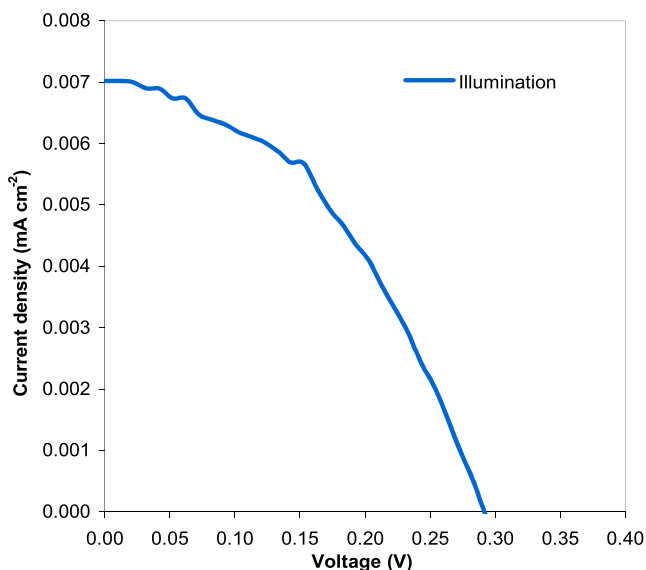
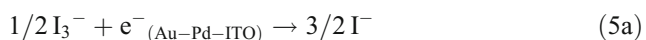
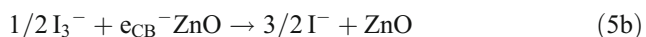


Fig. 10 *J-V* curve characteristic of DSSCs-based ITO-ZnO (N719 dye)/A1.0N0.2I/Au-Pd-ITO under illumination of 100 mW cm⁻²

continue the reduction reaction. Initially, the counter electrode obtained electrons from the external circuit of DSSCs. Thus, I₃⁻ was reduced to I⁻:



Once again, the reduction of I₃⁻ to I⁻ (Eq. 9a) must effectively compete with the charge-separated state during the recombination process (Eq. 9b) to avoid a decrease in current production in DSSCs:



Finally, the electrons released in the oxidation process enter the ZnO layer, and the circuit is completed. The D⁺ also returns to its origin form, D. This mechanism takes place continually as long as the DSSCs are exposed to the light.

The voltage produced by DSSCs in this work is based on the difference in energy levels between ZnO and the transition media (mediator) of I⁻/I₃⁻. It depends on the mediator and solvent used as well, besides the condition of the ZnO and the intensity of illumination. Agar paste GPE containing a mixture of (I⁻/I₃⁻) from NH₄I and I₂ serves as the charge carrier in the mediator. Meanwhile, the current produced by the cell is directly related to the amount of light absorbed by the dye. The amount of light here was fixed at 100 mW cm⁻².

Based on results, the agar paste demonstrated as a potential material for the DSSC electrolyte. Although

Table 4 *J-V* curve properties of DSSCs-based ITO-ZnO (N719 dye)/A1.0N0.2I/Au-Pd-ITO properties under illumination of 100 mW cm⁻²

<i>V</i> _{max} (V)	<i>J</i> _{max} (mA cm ⁻²)	<i>V</i> _{OC} (V)	<i>J</i> _{SC} (mA cm ⁻²)
0.17	0.005	0.29	0.007

ZnO electrode sensitized N-719 was a good semiconductor material for the DSSC working electrode, but the contact between ITO-ZnO (N719 dye) and A1.0N0.2I was not good in this work, lead to the low efficiency of the DSSC.

However, the physical properties of agar paste GPE (transparent slurry gel) give an advantage that improves the DSSC photophysical and redox reaction. This is due to the high conductivity of agar paste GPE (10⁻³ S cm⁻¹) in contrast with the low conductivity of solid polymer electrolytes (SPE) (10⁻⁶-10⁻⁴ S cm⁻¹) for DSSCs. Therefore, the value of *J*_{SC} is much higher compared with the other DSSC studies based on polysaccharides SPE (2–5 and 19.23 μA cm⁻²) [10, 24]. The *J-V* curve pattern is also similar to those reported in other studies on DSSCs [12, 42].

Conclusion

GPE-based agar paste + NH₄I + I₂ with various concentrations of redox electrolyte was prepared and characterized. Based on the GPE characterization analysis, agar paste+ 1.0 M NH₄I+0.2 μM I₂ (A1.0N0.2I) gave the highest conductivity (2.64±0.19)×10⁻³ S cm⁻¹, lowest viscosity (1.17±0.29) Pas and lowest activation energy of 0.25 eV. This sample had a good physical appearance compared with the other samples in term of transparency and mix well with NH₄I and I₂. The A1.0N0.2I was then successfully fabricated as a GPE for DSSCs with the combination of ITO-ZnO (N719 dye)/A1.0N0.2I/Au-Pd-ITO.

Acknowledgments SSA would like to thank MOSTI for the NSF scholarship and USM-RU-PRGS for grant no. 8031020. AAM is grateful for the financial support for the study provided by USM Short Term grant no. 6039030.

References

- Honda K, Fujishima A (1972) Nature 238:37
- O’Regan B, Gratzel M (1991) Nature 353:737–740
- Nazeeruddin MK, Kay A, Rodicio I, Humphry-Baker R, Mueller E, Liska P, Vlachopoulos N, Graetzel M (1993) J Am Chem Soc 115:6382–6390
- Saito M, Fujihara S (2008) Energy Environ Sci 1:280–283
- Hara K, Horiguchi T, Kinoshita T, Sayama K, Sugihara H, Arakawa H (2000) Sol Energy Mater Sol Cells 64:115–134
- Wang Y (2009) Sol Energy Mater Sol Cells 93:1167–1175
- Kubo W, Murakoshi K, Kitamura T, Yoshida S, Haruki M, Hanabusa K, Shirai H, Wada Y, Yanagida S (2001) J Phys Chem B 105:12809–12815
- Hara K, Arakawa H (2005) Dye-sensitized solar cells. In: Luque A, Hegedus S (eds) Handbook of photovoltaic science and engineering. Wiley, New York, pp 663–700
- Keis K, Magnusson E, Lindström H, Lindquist S-E, Hagfeldt A (2002) Sol Energy Mater Sol Cells 73:51–58

10. Mohamad SA, Yahya R, Ibrahim ZA, Arof AK (2007) *Sol Energy Mater Sol Cells* 91:1194–1198
11. Suzuki K, Yamaguchi M, Kumagai M, Tanabe N, Yanagida S (2006) *C R Chim* 9:611–616
12. Kaneko M, Hoshi T (2003) *Chem Lett* 32:872–873
13. Kaneko M, Hoshi T, Kaburagi Y, Ueno H (2004) *J Electroanal Chem* 572:21–27
14. Mohamad SA, Ali MH, Yahya R, Ibrahim ZA, Arof AK (2007) *Ionics* 13:235–240
15. Norman FS (2006) 2nd ed., CRC Press
16. Teramoto A, Fuchigami M (2000) *J Food Sci* 65:491–497
17. Cairns P, Atkins EDT, Miles MJ, Morris VJ (1991) *Int J Biol Macromol* 13:65–68
18. Piculell L, Borgström J, Chronakis IS, Quist PO, Viebke C (1997) *Int J Biol Macromol* 21:141–153
19. Ciancia M, Milas M, Rinaudo M (1997) *Int J Biol Macromol* 20:35–41
20. Wang W, Guo X, Yang Y (2011) *Electrochim Acta* 56:7347–7351
21. Yang Y, Hu H, Zhou C-H, Xu S, Sebo B, Zhao X-Z (2011) *J Power Sources* 196:2410–2415
22. Hara K, Horiguchi T, Kinoshita T, Sayama K, Arakawa H (2001) *Sol Energy Mater Sol Cells* 70:151–161
23. Maurya KK, Srivastava N, Hashmi SA, Chandra S (1992) *J Mater Sci* 27:6357–6364
24. Buraidah MH, Teo LP, Majid SR, Arof AK (2010) *Opt Mater* 32:723–728
25. Alias SS, Ismail AB, Mohamad AA (2009) *J Alloy Compd* 499:231–237
26. Al-Kahlout A, Vieira D, Avellaneda C, Leite E, Aegerter M, Pawlicka A (2009) *Ionics* 16:13–19
27. Wang M, Qi L, Zhao F, Dong S (2005) *J Power Sources* 139:223–229
28. Tan WC, Alias SS, Ismail AB, Mohamad AA (2011) *J Solid State Electrochem* :1–10
29. Bonhote P, Dias A-P, Papageorgiou N, Kalyanasundaram K, Gratzel M (1996) *Inorg Chem* 35:1168–1178
30. Kalaighan GP, Kang M-S, Kang YS (2006) *Solid State Ion* 177:1091–1097
31. Vieira DF, Avellaneda CO, Pawlicka A (2007) *Electrochim Acta* 53:1404–1408
32. Salihoğlu S, Tari Ö, Yurtseven H (2002) *Mater Chem Phys* 73:339–342
33. Renard I, Li H, Marsan B (2003) *Electrochim Acta* 48:831–844
34. Ueno H, Endo Y, Kaburagi Y, Kaneko M (2004) *J Electroanal Chem* 570:95–100
35. Wu J, Lan Z, Wang D, Hao S, Lin J, Huang Y, Yin S, Sato T (2006) *Electrochim Acta* 51:4243–4249
36. Ramesh N, Duda JL (2001) *J Membr Sci* 191:13–30
37. Saikia D, Kumar A (2005) *Eur Polym J* 41:563–568
38. Yue Z, McEwen IJ, Cowie JMG (2003) *Solid State Ion* 156:155–162
39. Mallik H, Sarkar A (2006) *J Non-Cryst Solids* 352:795–800
40. Calogero G, Marco GD (2008) *Sol Energy Mater Sol Cells* 92:1341–1346
41. Shobukawa H, Tokuda H, Tabata S-I, Watanabe M (2004) *Electrochim Acta* 50:305–309
42. Philiat JM, Marsan B (1999) *Electrochim Acta* 44:2915–2926